Evaluation of Flexural Behavior and Service Condition of GFRP and CFRP Hybrid Reinforced Concrete Beams

Abd El Rahman. Megahid[1], Omar. A. Farghal[2], Hossam El Din Mohamed[3], Mohamed Ahmed Seif El-Din[4]
Mohaseb. A. Abozied[5]

[1] Abd El Rahman Megahid (Professor of Structural Engineering, Assiut University, Egypt)
[2] Omar. A. Farghal (Professor of Structural Engineering, Assiut Universit, Egypt)
[3] Hossam El Din Mohamed (Lecturer of Structural Engineering, Assiut University, Egypt
[4] Mohamed Ahmed Seif El-Din (Lecturer of Structural Engineering, Assiut University, Egypt
[5] Mohaseb.A.Abozied (Ass. Lecturer of Structural Eng, Higher Institute of Eng. Luxor. Egypt

Abstract – Through theoretical and experimental research this study investigates the flexural behaviour of hybrid bar-reinforced concrete beams under static load. The dimensions of each beam are 150 x 250 x 2036 mm. All of the examined beams underwent four-point loading testing. Steel has been replaced by fibre-reinforced polymer (FRP) bars for RC elements exposed to those environments. Many experts have focused their emphasis on conducting numerous studies on various types of FRP products due to its non-corrosive nature. Numerous standards have also been developed as a result of extensive investigation. In this context, a novel FRP material combination is investigated in this study, and its properties are derived. In this study, carbon and glass fibres combine to create a novel hybrid rebar. Alternative solutions, such as using a hybrid reinforcement (CFRP rods and GFRP bars) as a principal reinforcement, have been suggested as a way to enhance the structural performance of GFRP reinforced concrete members. Even stronger than steel in terms of tensile strength and elastic modulus is carbon fibre. These are benefits of employing carbon fibre from a structural perspective, but not from an economic one because of how much more expensive it is than glass fibre. To address the inadequacies of the FRP rebar, the idea of "hybridization" was developed. FRP bars' mechanical characteristics can allow for significant deflections and crack widths. As a result, the serviceability limit states are frequently used to guide the design of concrete elements reinforced with FRP materials (SLS). The study's primary factors include the reinforcement ratio, and the hybridization ratio of CFRP to GFRP (CFRP / (CFRP +GFRP)). Deformations of the reinforcement and concrete, as well as crack width and spacing, are measured and studied. The experimental findings are presented and contrasted with some of the most accurate deflection and cracking prediction models for steel and FRP RC. In this study, there was an improvement in the elasticity parameters by 87%, an improvement in tensile strength by 11.6%, and an improvement by 63% in the elongation ratio.

Keywords: hybridization, flexural, serviceability, elastic modulus, higher tensile strength

1. INTRODUCTION

Fibre reinforced polymer (FRP) bars have started to be employed for internal longitudinal flexural reinforcement (FIB 2007) [10]. Continuous fibres contained in a polymeric matrix make

up FRPs, a type of composite material. Typically, these composites are divided into three categories based on the type of fibre used: (GFRP), (CFRP), and (AFRP). Because FRP bars are non-corrosive, using them can lower maintenance and rehabilitation expenses, which has positive effects on the economy and the environment (Pilakoutas et al. 2007) [20]. Additionally, when it's crucial to avoid magnetic field interference, FRP bars might be employed because of their magnetic neutralityBridges are an example of a location where applications or demonstration projects have been successfully completed., chemical facilities, coastal habitats, and highway infrastructure (Nanni 2001[19], Hollaway 2010[11]). One example of how such specialised properties might lead to new uses is the use of diaphragm walls in temporary applications, for which the high cuttability of FRPs is a major asset (Fib 2007[10], Pilakoutas et al. 2007[20]). FRP bars are projected to perform structurally differently when used due to their differing mechanical and link properties from those of steel rebar, specifically their relatively low modulus of elasticity and their linear stress-strain behaviour till failure.

Huge strains can be generated in FRP bars at low levels of external loads due to their lower stiffness, which can result in large fracture widths and deflections .The design of concrete elements reinforced with FRP materials is generally determined by the serviceability limit states (SLS), as GFRP typically only has an elastic modulus of 35 to 45 GPa (Matthys and Taerwe 2000[15], for example). Nanni 2003[16]). Masmoudi R, Thériault M, and Benmokrane B[14], Brown VLand, Benmokrane B[3], ISIS 2001 [12], and Branson's equation, which is utilised in steel design regulations [8], has been modified by coefficients suggested by Bartholomew CL[6], Pecce M et al. 200[21], Toutanji HA, and Saafi M[22]. According to [Bischoff PH 2005[4] and Faza, et al., a modified equivalent moment of inertia derived from curvatures has been provided. 1992[9] for deflections in the state of serviceability. Several design guideline proposals for FRP RC ACI Committee 318 from 2005[1], Hollaway and L. C. from 2010,[11], and ACI Committee 440 from 2006[2] have used these various techniques.

GFRP reinforcing rods are non-corrosive, lightweight, high tensile, electromagnetic, and fatigue endurance, giving them considerable benefits over steel reinforcement. The drawbacks of FRP rods include their high cost, lack of yielding prior to brittle rupture, low transverse strength, challenging anchorage techniques, poor adhesion to concrete, and in some forms, lower elastic modulus than steel bars. Some GFRP rods' low elasticity modulus is a major reason for concern, placing a lot of attention on the serviceability of the reinforced structures. In the tension zone, it frequently causes an increase in deflections, crack width, and crack propagation. When employing GFRP rods in concrete flexural members, designers are also concerned that there won't be any yielding, which could cause brittle collapse. One approach to solving these issues is to use both GFRP and CFRP rods to support the concrete members. There is still room for improvement in this new reinforcing method, and further study is required. An experiment will be carried out to shed some light on the flexural behaviour of concrete beams reinforced with hybrid reinforcement (CFRP rods and GFRP rods) or just with (GFRP) rods.

2. Experimental programme
2.1. Beam specimen
Analysing the effects of changing the hybridization ratio and reinforcing ratio of FRP RC beams was the experimental program's objective. Each beam has a 150 x 250 mm rectangular cross-section and a 2036 mm overall length. The specimens underwent four-point bending testing with a 3.2 ratio of shear span to depth. Below is a description of the specimens, materials, test setup, and equipment in detail.

2.2 FRP Reinforcement.

Glass fibre reinforcement and hybrid fibre reinforcement made of glass and carbon bars, respectively, were employed as FRP reinforcement bars. Table 1 lists the nominal diameters for bars. The FRP reinforcement bars' nominal specifications include their assured rupture strain, elastic modulus, and tensile strength . To strengthen the bond with the surrounding concrete, all bars utilised in this experimental programme have a ribbed surface, with the exception of mild steel (8mm). The three FRP reinforcement bars are shown in Figure 1.

FIGURE 1: FRP bars used in this study

Table 1. Results of tensile tests for three average values of specimens.

Specimen Type	Actual bar diameter (mm)	Yield tensile stress or proof stress (MPa))	Ultimate tensile strength (MPa))	Elastic modulus GPa)	Ultimate strain %	Modulus Of Toughness *(Mpa)*
GFRP bar	8.1	--------	1240.6	47	2.64	٩٥٠
Hybrid (GFRP+ CFRP) bar	8.1	--------	1384.5	88	1.65	١٢٤٠
CFRP bar	7.99	---------	1730	120.8	1.43	1070
8mm- steel bar	7.9	248	355	200	22	612

2.3 Preparation of Cages

This research's main objective was to examine how FRP RC beams behaved in terms of serviceability. Stress, cracking, and deflections were therefore meant to be recorded for the various beam specimen types. In more detail, the hybridization ratio was used to analyses how these beams

affected the particles . Four-point bending static loading was used to evaluate the FRP RC beams. The primary variable for longitudinal reinforcement varies depending on the ratio of glass to carbon fibre hybridization (25, 50, 35,65and 75 percent , respectively). Table 2 and Figure 2 both display the reinforcing information for the examined beams.
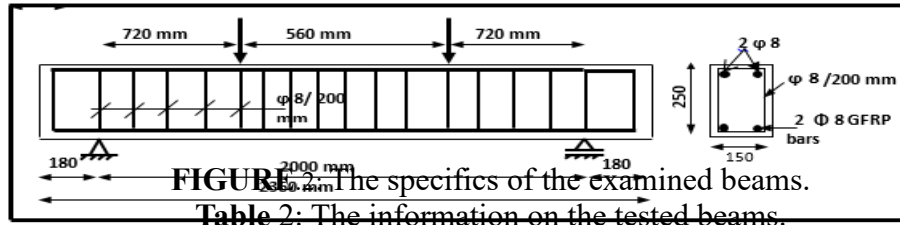

FIGURE 2: The specifics of the examined beams.

Table 2: The information on the tested beams.

Study Parts	examined Beam No.	F_u MPa	a/d	FRP bars Reinf.	Steel Bars Reinf	ρ_f %	A_c / A_c +AG	Vertical steel stirrups Reinf.
	A1G	38.5		2Φ8	----	0.298	------	
Group D	D1GC	38.5	3.2	٧5%CFRP ٢5% GFRP	-----	0.298	.75	
	D2GC			٢5%CFRP ٧5% GFRP			.25	
	D3GC			35%CFRP 65% GFRP			.35	
	D4GC			65%CFRP 35% GFRP			.65	
	D5GC			50%CFRP 50% GFRP			.5	

After the strain gauges in the middle of the beams were fitted, the FRP reinforcement cages were positioned and lowered into the formwork. The interiors of the cages were oiled to make removal easier after the concrete had been cast and had a chance to cure. The cages for the FRP reinforcement were precisely centered. Before pouring the concrete, fasten the strain gauges to avoid damaging the wires. as illustrated in Figure 3, a timber frame was drilled across the formwork. To avoid causing any harm to the strain gauges, vibration was applied cautiously and carefully around them. After pouring, In order to create a flat, smooth surface, the concrete was polished and troweled. After pouring concrete into the concrete cubes in three layers, the FRP RC beams were taken out to provide room for the installation of concrete strain gauges. according to Figure 3-36

FIGURE 3: Concrete Pouring of Test Specimens

2.3 Test Procedure

These beams were put through a static load test when they were 28 days old. At the start and the conclusion of each increment of loading for all tested beams, readings from the electrical

strain gauges for beams with web reinforcement, LVDT It was placed in the middle of the beams which use for deflection, and the crack growth was observed. The tests were carried out until the beam failed or the load reading significantly decreased. according to figure 4.


Fig. 4 Schematic view of the test setup

3. Test results and discussions
3.1 Results and discussion

　　　With the aid of a magnifying lens, the beginning and growth of cracks for the various tested beams were seen visually. It was observed that the cracks on both sides of all the beams were roughly the same. The first crack that was seen reached a height higher than half of the beam depth. These cracks enlarged and spread upward as the load grew. Later, fresh cracks were developed at the bottom of the beam, and those formed cracks spread in the direction of the place where the load was applied. The crack spacing, which is comparable to stirrup spacing, is clearly shown in Figure 5 to have been distributed consistently along the beams reinforced with FRP bars. This confirms the findings of Faza and Gangarao in 1992 [9]. The tendency of the fractures to form where the stirrups were was due to the lack of link between the FRP bars and the concrete. By extending the contact area between the longitudinal GFRP reinforcements and the concrete, transverse reinforcements would narrow the crack spacing. The pace at which stress is transferred from the reinforcements to the concrete would rise as a result. Table 3 reports the first crack, crack spacing, crack number, and crack breadth. Figures 5 and 6 illustrate these parameters.

3.2. Effect of Hybridization Ratio of FRP bars (ρ_{fh} %)

　　　The impact of the hybridization ratio on the beam fracture patterns (D1GC, D2GC, D3GC, D4GC and D5GC).The number and the height of cracks at the same level of loading were decreased as the carbon ratio in FRP bars increased. In addition, the higher carbon ratio in beams gives a smaller crack width at the same loading condition. The mode of failure of all beams in this series were flexural and concrete crushing. Increasing the carbon ratio (from 25% to 75%) improving the cracking behavior. It reduced the number of crack (from 12 to 9) also the spacing of cracks decrease (from 18 to 15 cm) and the crack width reduced (from 1.2 mm to .75mm).
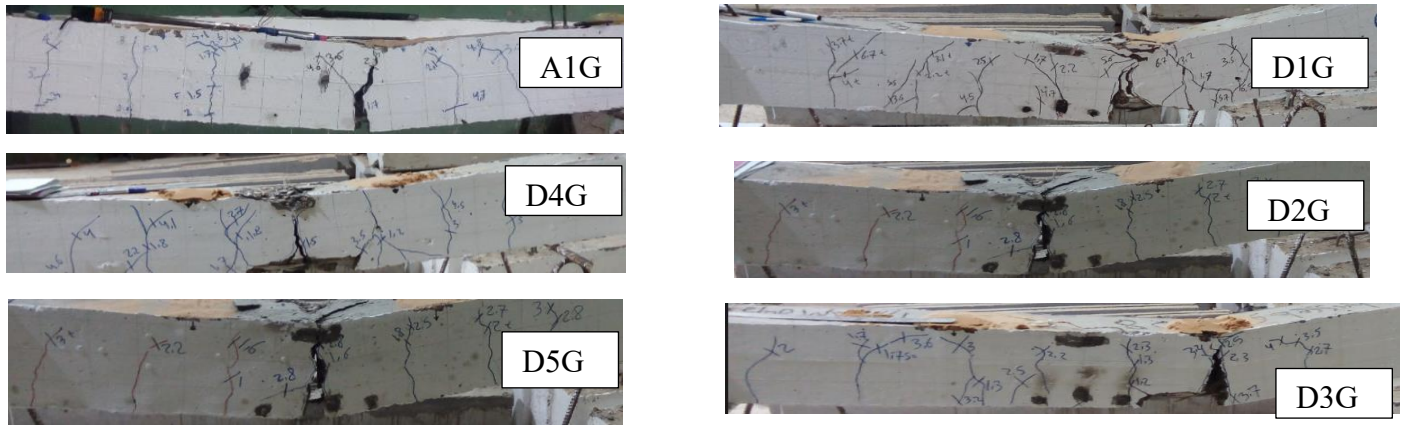
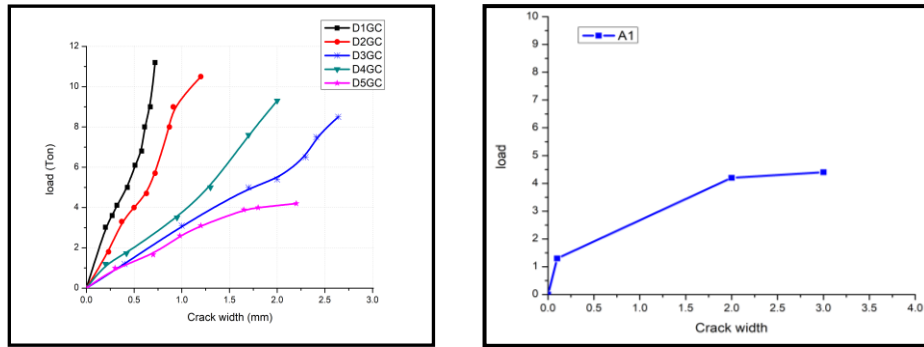**FIGURES.** 5: Mode of failure and the crack pattern for the tested beams

FIGURE 6: Effect of Hybridization Ratio of FRP bars *(ρ$_{fh}$ %)* on crack Widt
Table 3Details of cracks for all tested beams.

Beam Identification	Ultimate Load (ton)	Service Load (ton) *At cracking limitation (.5-.7)mm*	First Crack Load (ton)	Total Number of Cracks	Average Crack Spacing (mm)
A1G	4.5	4	1	٧	200
D1GC	11.5	-----	1.5	٩	160
D2GC	10.5	6.7	1.5	١٧	170
D3GC	8.5	2.4	1.5	١١	180
D4GC	9.5	2.4	1.5	١٢	180
D5GC	5.5	1.9	1.5	٨	200

3.3. Service load

The limitations that are reached at the lowest load value serve as the regulating parameters for the service limit state (SLS). At the lowest load value, the SLS, which has been researched, approaches its limits. The SLS under investigation are: ·
Service load According to Stresses on materials : 45 % of the compressive strength fc is the

maximum allowable compressive stress for concrete. The service load is the weight at which the mid-span section's top strain gauge registers the maximum concrete compressive strain as follows:

$$\varepsilon_C = 0.45 \, f_{cu} \, / \, E_C \qquad (1)$$

Only tested beams with strain gauges affixed to the concrete surface are the subject of this data. · **Service load According to Crack width**: The largest crack can only be from 0.5 to 0.7 mm wide.
The Crack width at which the largest crack, as measured at the height of the reinforcement in the central zone, equals the service load.:

$$w \max = \, {}_{,}0.5 - 0.7 \, mm \qquad (2)$$

· **Service load According to Deflection**: Span of beam/250 limited of the deflection. The load at which the vertical transducer measures the instantaneous experimental mid span deflection is known as the service load.

$$\mu \, mid \, span = L \, /250 \qquad (3)$$

The cracking load and the ultimate load are connected to for comparison purposes, the obtained service load Ps for each SLS is shown in table4.
Service load According to Strain on materials:

ISIS 2001 [12] defines the PS as the load that causes a tensile strain of 2000 µε in the reinforcement.

Service load According to Ultimate load:
According to Bischoff et al2008 .'s [5] suggestion, the PS should be around 30% of the beam's ultimate load at failure (0.3Pu). With the exception of (A0), all beams are strengthened with FRP bars. , recorded comparable $P_{s \, exp}$ values. Based on this criterion, see Table 4 and Table 5

Table 4. Experimental value of service and ultimate loads for all tested beams

Beam ID	P_S (ton)						P_U (ton)	Failure mode	P_S / P_U
	.3Pu	*At 2000µε*	*L /250*	*.45 F_{CU}*	*W(.5-.7)mm*	*P_{S*} (ton)*			
A1G	1.35	1.25	1.65	.4	4	1.25	4.5	FC	0.28
D1GC	3.45	2.75	7.8	4.7	-----	2.75	11.5	FC	0.24
D2GC	3.15	1.75	4.9	2.5	6.7	1.75	10.5	FC	0.17
D3GC	2.55	1.2	3.2	2.6	2.4	1.2	8.5	FC	0.14
D4GC	2.85	1.5	6.7	3.2	2.4	1.5	9.5	FC	.016
D5GC	1.65	1.3	---------	1.78	1.9	1.3	5.5	FC	0.24

Where , F: flexural, FC: flexural compression
P_s*: is the smallest value of experimental values of P_S limitations.

Table 5. Experimental value of cracking and ultimate loads for all tested beams.

Beam No.	P_{cr} (ton)	P_u (ton)	P_{cr}/P_u
A1G	1	4.5	0.22
D1GC	1.5	11.5	0.134
D2GC	1.5	10.5	0.143
D3GC	1.5	8.5	0.18
D4GC	1.5	9.5	0.16
D5GC	1.5	5.5	0.27

Where P_{cr}- cracking load - P_u-ultimate load

3.4. Load – Deflection Behavior

Utilizing information from the LVDT machine in the central zone, the deflection is calculated. For each of the different tested beams , the measured mid-span deflection values at the bottom surface were plotted versus the active flexural load applied until failure. Figure 7 depicts the experimental mid span load-deflection relationship of FRP RC beams.
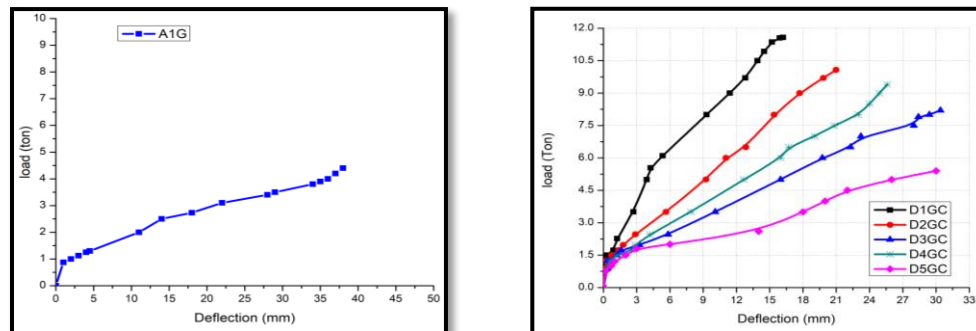

FIGURE 7: Relationships of Load – deflection for beams.

The effective moment of inertia noticeably decreases as soon as the concrete in the tension zone of the concrete beam cracks, which causes the section's stiffness to decrease. For beams (D1GC, D2GC, D3GC,D4GC, and D5GC), the carbon fiber content in the composite fibers is 75%, 25%, 35%, 65%, and 50%, respectively. It was observed that the deflection decreased as the carbon ratio increased (from 30.4mm to 16.2mm). This reduction in deflection was brought about by strengthening the beams with CFRP, a material with high elastic modules and high tensile strength. The flexural load-deflection curve then started to vary and flatten out, though it remained still linear. At the maximum moment zone, cracking developed as the applied stress increased. when the applied stress is more than the cracking load, resulting in a loss of stiffness.

 4. Strain

4.1. Concrete strain

The experimental load-concrete compressive strain relation is illustrated by local strain gauges at the center of Figure 8.
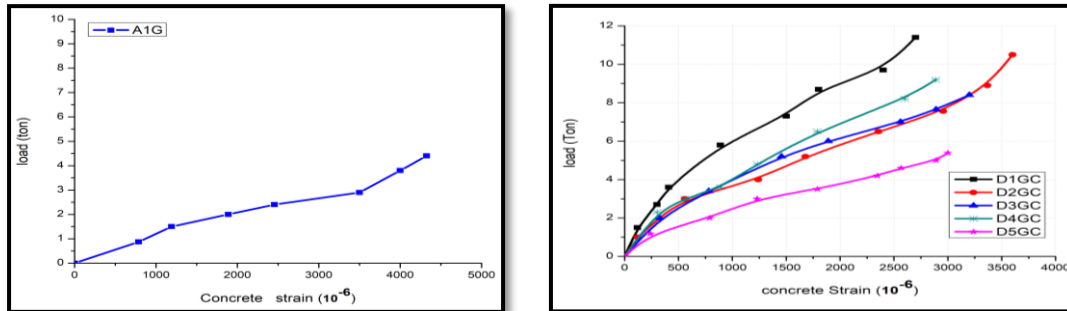
FIGURE 8: Load-strains on the concrete beams' upper surface

4.2. Strain in rebar.

For the various beams tested under static load, the tensile strain in the major longitudinal reinforcement was measured at mid-span. The hybrid reinforcement used in the tested beams (GFRP and CFRP bars) was slightly smaller than that used in the control beam (A1G), as seen in figure 9. This is caused by the GFRP bars in the control beams' low elastic modulus. The elastic modulus is improved by the carbon ratio. The c/d at service state and failure were calculated using the measured strains (see Table 6). The neutral axis's location did not vary noticeably between the service state and failure, and the c/d did not considerably alter between the service state and failure, indicating that the portions were completely cracked. Additionally, when the reinforcement ratio grew, so did the neutral-axis depth.
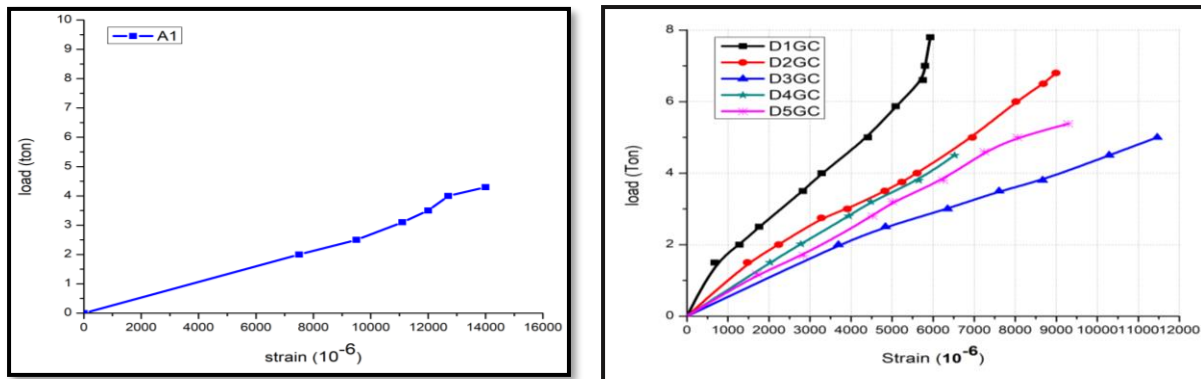

FIGURE 9: Reinforcement strain relationships on beams

Table shows the estimated curvature at failure (ult) and at service state (s) (6). Jaeger et al. (1995) [13] created the concept of deformability in order to quantify this deformation feature and give a mechanism to compare the level of safety between the ultimate and service states. The deformability of sections reinforced with FRP is assessed using a "deformability factor," as stated in Equation 9.1, in accordance with Jaeger et al. (1995) [13]. The quantities uMs stand in for the curvature and moment at service. According to CAN / CSA. (2012) [8] and CAN /CSA. (2012) [7], the service state is the strain state that corresponds to a maximum compressive strain in concrete of 0.001. The deformability factor must be greater than 4 or 6, respectively, for rectangular and T-sections. According to Newhook et al. (2002) [17], the numbers uMs should correspond to the actual service limit condition. Additionally, they offered a technique for using the FRP's limiting service strain values as the basis for deformability-based design. . deformability factor $= \frac{\Psi u \times Mu}{\Psi s \times Ms}$

(4)

Curvature factor $\quad = \frac{\Psi u}{\Psi s}$ (5)

$$\Psi_u = \frac{\varepsilon_c}{C}, \tag{6}$$

$$C = \left(\frac{\varepsilon_c}{\varepsilon_c + \varepsilon_{frp}}\right) * d \tag{7}$$

$$\Psi_s = \frac{\varepsilon_c}{Kd} = \frac{0.001}{Kd} \qquad \varepsilon_c = \text{stress at ultimate} \tag{8}$$

The subscripts (u) and (s), respectively, represent service limit states and ultimate limit states. , where (M) is the bending moment and (Ψ) is the curvature. Effective depth, in (mm), ultimate strain in concrete under compression, and k stress decay factor, taken as 1.0 for (c/o1.0) and as a quantity greater than 1.0 for (c/o>1.0) (f frpu) FRP's maximum tensile strength is MPa (Efrp) and its elasticity modulus is MPa.

4.3. Neutral-Axis Depth
The experimental neutral axis was located using the data from the concrete strain gauges. Table 6 demonstrates that the neutral-axis depth was slightly lower after breaking because the difference between the service and failure neutral-axis depths is not particularly great. As the reinforcement ratio increased, the neutral-axis depth increased as well. In order to handle the higher forces brought on by larger reinforcement areas, a larger compression block is required for the forces to be in equilibrium. The theoretical neutral-axis depth was determined using the cracked-section analysis given in Eq. The theoretical prediction and the experimental results show good agreement.

$$\frac{C}{d} = \sqrt{2\rho_f n_f + \left(2\rho_f n_f\right)^2} - 2\rho_f n_f \tag{9}$$

Table 6: Strains, neutral axis-to-depth ratio, and curvature of FRP-RC beams

Beam No.	Reinforcement Strain (με)		Concrete Strain (με)		c/d)exper.		Curvature, Ψ		Deform. factor (J)
	Service	Failure	Service	Failure	Service	Failure	Curvature Ψ_s	Curvature, Ψ_u	$\Psi_u * M_u / \Psi_s * M_S$
A1G	5000	14000	1100	3100	0.18	0.18	91.06	76.00	4.64
D1GC	2800	5800	450	2600	0.14	0.31	35.87	37.33	7.98
D2GC	4000	9000	650	3600	0.14	0.29	51.81	56.00	7.57
D3GC	6100	11500	750	3250	0.11	0.22	68.77	65.56	5.40
D4GC	3800	6500	480	2800	0.11	0.30	44.01	41.33	5.95
D5GC	2000	11000	600	3000	0.24	0.24	8.73	55.56	4.53

Where (Ψ) is the curvature, the subscripts(u) and (s) refer to ultimate limit states and service limit states,(c/d) is the neutral axis-to-depth ratio.

5. Ductility.
Based on structural factors such mid-span deflection, curvature, or energy absorption capacity as shown by the area under the load-deflection curve, the ductility of reinforced concrete beams can be determined. The maximum deflection [max] equal to 90% of the ultimate load and the deflection associated with the cracking load [cr] were used to construct the displacement ductility index [μ_D] that was taken into account. The displacement ductility index [D] for each of the tested beams is displayed in Table 7.

Table 7. Experimental and predicted cracking and ultimate loads

Beam No.	A_C / $(A_C + AG)$	P_f	Ductility		
			Δmax (mm)	Δ_{Cr} (mm)	μ_D
A1G	-----	0.298	38	1	38
D1GC	.75		16.2	1.1	14.72
D2GC	.25		20.99	1.2	17.5
D3GC	.35	0.298	30.4	1.4	21.7
D4GC	.65		25.6	1.3	19.7
D5GC	.5		30	1.6	18.75

In contrast, a structure's ductility refers to its capacity to absorb energy absorption without breaking. Naaman and Jeong (1995[18]) It was estimated by measuring the region under the load-deflection graph for the FRP RC beams under static loading, as illustrated in Table 8. Table

Table 8: Energy Absorption Capacities of FRP RC Beams

Beam No.	A1G	D1GC	D2GC	D3GC	D4GC	D5GC
energy absorption capacity (t.m)	104.5	112	78	56	45	88

6. Conclusions

-In comparison to beams reinforced with hybrid FRP, those reinforced with FRP bar only showed higher deflection values at any load level up to failure (CFRP and GFRP).
 -Only a greater crack width and space of cracks are visible in GFRP-reinforced beams compared to those reinforced with hybrid (GFRP and CFRP) bars.
-The trial outcomes demonstrated that the lowest load value corresponded to around 2000 bars.
-Although concrete crushing caused all of the beams to fail, a considerable degree of deformability was reached prior to collapse. The computed deformability factor was greater than 4 in each example.
The average crack spacing of RC beams is the shortest, that of FRP RC beams is the largest, and that of hybrid RC beams is in the middle when subjected to the same loading. When ACFRP/(ACFRP+AGFRP) drops with the same ultimate bearing capacity and stresses, the average fracture spacing decreases.
-Beams reinforced with GFRP rods only exhibit a 50 percent reduction in stiffness and ductility compared to beams strengthened with hybrid reinforcement or composite reinforcement; this is because these beams have huge crack widths and rapid deformation rates.

REFERENCES

[1] ACI Committee 318. Building code requirements for structural concrete and commentary (ACI 318-05/ACI 381R-05). Detroit, Michigan (USA): American Concrete Institute; 2005.

[2] ACI Committee 440. Guide for the design and construction of concrete reinforced with FRP Bars (ACI 440.1R-06), Farmington Hills, Michigan (USA): American Concrete Institute; 2006.

[3] Benmokrane B, Chaallal O, Masmoudi R. Flexural response of concrete beams reinforced with FRP reinforcing bars. ACI Struct J 1996;91(2):46–55.

[4] Bischoff PH. Reevaluation of deflection prediction for concrete beams reinforced with steel and fiber-reinforced polymer bars. J Struct Eng 2005;131(5):752–67.

[5]Bischoff, P. H., and Johnson, R. D. (2008). "Effect of shrinkage on short-term deflections of reinforced concrete beams and slabs." ACI Structural Journal, 105(4), 516-518.

[6] Brown VL, Bartholomew CL. Long-term deflection of GFRP reinforced concrete beams. In: Fiber Composites in Infrastructure. Proceedings of the 1st international conference on composites in infrastructures (ICCI/96); 1996. p. 389–400.

[7] CSA Standard CAN/CSA-S806-02. Design and construction of building components with fiber-reinforced polymers. Mississauga, Ontario, Canada: Canadian Standards Association; 2002.

[8]CAN/CSA. (2012). "CAN/CSA-S806. Design and construction of building components with fiber-reinforced polymers." Canadian Standards Association, Ontario, Canada, 177p.

[9]Faza, S. S., and GangaRao, H. V. S. (1992). "Pre- and post-cracking deflection behaviour of concrete beams reinforced with fibre-reinforced plastic rebars." Proceedings of The First International Conference on the Use of Advanced Composite Materials in Bridges and Structures, K.W. Neale and P. Labossière, Editors; Canadian Society for Civil Engineering, 1992, 151-160.

[10] Federation International du Beton, FIB, Task Group 9.3. FRP reinforcement in RC structures, Lausanne, Switzerland; 2007

[11] Hollaway, L. C. (2010). "A review of the present and future utilization of FRP composites in the civil infrastructure with reference to their important in-service properties." Construction and Building Materials

[12] ISIS Canada. Reinforcing concrete structures with fiber-reinforced polymers – design manual no. 3, Manitoba, Canada: ISIS Canada Corporation; 2001.

[13]Jaeger, L.G., Tadros, G., Mufti, A.A. (1995). "Balanced Section, Ductility and Deformability in Concrete with FRP Reinforcement." Research Report presented in Joint U.S.-Canadian Meeting at West Virginia University.

[14] Masmoudi R, Thériault M, Benmokrane B. Flexural behavior of concrete beams reinforced with deformed fiber reinforced plastic reinforcing rods. ACI Struct J 1998;95(6):665–76.

[15]Matthys, S., and Taerwe, L. (2000). "Concrete slabs reinforced with FRP grids. I: One-way bending." Journal of Composites for Construction, 4(3), 145-153.

[16]Nanni, A. (2003). "North American design guidelines for concrete reinforcement and strengthening using FRP: Principles, applications and unresolved issues." Construction and Building Materials, 17(6-7), 439-446.

[17]Newhook, J., Ghali, A., and Tadros, G. (2002). "Concrete flexural members reinforced with fiber reinforced polymer: Design for cracking and deformability." Canadian Journal of Civil Engineering, 29(1), 125-134.

[18]Naaman, A.E., Jeong, S.M. (1995). "Structural Ductility of Concrete Beams Prestressed with FRP Tendons." Proceedings of the 2nd International RILEM Symposium (FRPRCS-2), Non-metallic (FRP) Reinforcement for Concrete Structures, Nawy,

[19]Nanni, A. (2001). "Relevant field applications of FRP composites in concrete structures."

Composites in Construction, Porto, Portugal, October 10-12, 2001,

[20]Pilakoutas, K., Guadagnini, M., Neocleous, K., and Taerwe, L. (2007). "Design guidelines for FRP reinforced concrete structures." Proceedings of the Advanced Composites in Construction, University of Bath, Bath, UK.

[21] Pecce M, Manfredi G, Cosenza E. Experimental response and code models of GFRP RC beams in bending. J Compos Constr 2000;4(4):182–90

[22] Toutanji HA, Saafi M. Flexural behavior of concrete beams reinforced with glass fiber-reinforced polymer (GFRP) bars. ACI Struct J 2000;97(5):712–9